Journal of Physics: Conference Series **381** (2012) 012016 doi:10.1088/1742-6596/381/1/012016

Supernova Dynamics and Explosive Nucleosynthesis

Karlheinz Langanke

GSI Helmholtzzentrum für Schwerionenforschung, Darmstadt, Germany
Institut für Kernphysik, Technische Universität Darmstadt, Darmstadt, Germany
Frankfurt Institute for Advanced Studies, Frankfurt, Germany

E-mail: k.langanke@gsi.de

Abstract. Nuclear physics plays a crucial role in various aspects of core collapse supernovae. The collapse dynamic is strongly influenced by electron captures. Using modern many-body theory improved capture rates have been derived recently with the important result that the process is dominated by capture on nuclei until neutrino trapping is achieved. Following the core bounce the ejected matter is the site of interesting nucleosynthesis. The early ejecta are proton-rich and give rise to the recently discovered νp-process. Later ejecta might be neutron-rich and can be one site of the r-process. The manuscript discusses recent progress in describing nuclear input relevant for the supernova dynamics and nucleosynthesis.

1. Introduction

Only a few years after Rutherford discovered the atomic nucleus and established 'nuclear physics', Eddington already conjectured that what was possible in Rutherford's laboratory 'may not be too difficult in the Sun.' Indeed due to the work of Hans Bethe, Willy Fowler and many others we know now that our Sun - like all other stars - generate the energy, necessary to exist in hydrostatic stellar equilibrium and to shine for millions to billions of years, by nuclear reactions in the stellar interior. For most of the reactions involved we have yet not been able to measure the relevant cross sections at the energies at which they occur in stars, and if one succeeded one had to go to deep underground environments like the LUNA facility with strongly reduced backgrounds. These measurements have been true highlights of modern nuclear astrophysics. The earthbound observation of the neutrinos generated by the reactions of solar hydrogen burning has proven the existence of neutrino oscillations, but has also confirmed our general understanding of the Sun, although small deviations to the sound-speed determination by helioseismology remain. Compilations of the solar reaction cross sections can be found in [1, 2]. It is desirable if the deviations between the measured [3, 4] and expected [5] electron screening enhancement of low-energy reaction cross sections, which is currently hampering some direct laboratory measurements, were removed.

Because of the larger charge, helium, the ashes of hydrogen burning, cannot effectively react at the temperature and pressure present during hydrogen burning in the stellar core. After exhaustion of the core hydrogen, the resulting helium core will gravitationally contract, thereby raising the temperature and density in the core until these are sufficient to ignite helium burning, starting with the triple-alpha reaction, the fusion of three ^{4}He nuclei to ^{12}C, followed by the famous $^{12}C(\alpha,\gamma)^{16}O$ reaction. In massive stars, this sequence of contraction of the core nuclear ashes continues until ignition of these nuclei in the next burning stage repeats itself several

times. After helium burning, the massive star goes through periods of carbon, neon, oxygen, and silicon burning in its central core. At this stage the temperature in the stellar core has reached values of a few 10^9 K which is sufficient to bring nuclear reactions mediated by the strong and electromagnetic interaction into equilibrium with its inverse. As a consequence, the nuclear composition is given by Nuclear Statistical Equilibrium (NSE) which, for proton-to-neutron ratios close to unity, favor nuclei in the mass range near iron which have the highest binding energy per nucleon. Moreover, the nuclear energy source for the star ceases, resulting in a collapse of the stellar core and an explosion of the star as a type II supernova. The nuclear physics associated with this cataclysmic event is the focus of the rest of this manuscript.

2. A short description of core-collapse supernovae

Massive stars end their lifes as type II supernovae, triggered by a collapse of their central iron core with a mass of more than $1M_{\odot}$. The general picture of a core-collapse supernova is probably well understood and has been confirmed by various observations from supernova 1987A. It can be briefly summarized as follows:

At the end of its hydrostatic burning stages, a massive star has an onion-like structure with various shells where nuclear burning still proceeds (hydrogen, helium, carbon, neon, oxygen and silicon shell burning). However, the iron core in the star's center has no nuclear energy source to support itself against gravitational collapse. As mass is added to the core, its density and temperature raises, finally enabling the core to reduce its free energy by electron captures of the protons in the nuclei. This reduces the electron degeneracy pressure and the core temperature as the neutrinos produced by the capture can initially leave the star unhindered. Both effects accelerate the collapse of the star. With increasing density, neutrino interactions with matter become decisively important and neutrinos have to be treated by Boltzmann transport. Nevertheless the collapse proceeds until the core composition is transformed into neutron-rich nuclear matter. Its finite compressibility brings the collapse to a halt, a shock wave is created which traverses outwards through the infalling matter of the core'e envelope. This matter is strongly heated and dissociated into free nucleons. Due to current models the shock has not sufficient energy to explode the star directly. It stalls, but is shortly after revived by energy transfer from the neutrinos which are produced by the cooling of the neutron star born in the center of the core. Neutrinos carry away most of the energy generated by the gravitational collapse and a fraction of the neutrinos are absorbed by the free nucleons behind the stalled shock. Multi-dimensional supernova simulations show that plasma instabilities and convection play crucial roles in the explosion mechanism as well. The revived shock can then explode the star and the stellar matter outside of a certain mass cut is ejected into the Interstellar Medium. Due to the high temperatures associated with the shock's passage, nuclear reactions can proceed rather fast giving rize to explosive nucleosynthesis which is particularly important in the deepest layers of the ejected matter. Reviews on core-collapse supernovae can be found in [6, 7].

3. Electron capture and its influence on the collapse

During most of the collapse the equation of state is given by that of a degenerate relativistic electron gas [6]; i.e. the pressure against the gravitational contraction arises from the degeneracy of the electrons in the stellar core. However, the electron chemical potential at core densities in excess of 10^8 g/cm^3 is of order MeV and higher, thus making electron captures on nuclei energetically favorable. As these electron captures occur at rather small momentum transfer, the process is dominated by Gamow-Teller transitions; i.e. by the GT$_+$ transitions, in which a proton is changed into a neutron. When the electron chemical potential μ_e (which grows with density like $\rho^{1/3}$) is of the same order as the nuclear Q-value, the electron capture rates are very sensitive to phase space and require a description of the detailed GT$_+$ distribution of the nuclei involved which is as accurate as possible. Furthermore, the finite temperature in the star requires

the implicit consideration of capture on excited nuclear states, for which the GT_+ distribution can be different than for the ground state. It has been demonstrated [8, 9] that modern shell model calculations are capable to describe GT_+ distributions rather well [10] (an example is shown in Figure 1) and are therefore the appropriate tool to calculate the weak-interaction rates for those nuclei ($A \sim 50 - 65$) which are relevant at such densities [11].

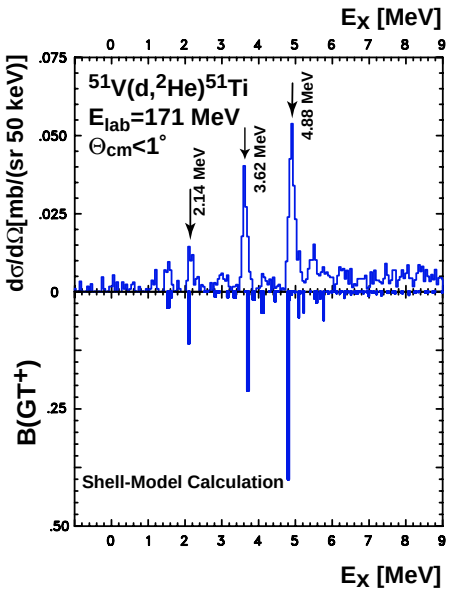

Figure 1. Comparison of the measured ^{51}V(d,^{2}He)^{51}Ti cross section at forward angles (which is proportional to the GT_+ strength) with the shell model GT distribution in ^{51}V (from [12]).

In a very recent landmark experiment, the GT strength has been measured for the unstable nucleus ^{56}Ni [13]. Besides establishing charge-exchange measurements performed in inverse kinematics, which opens the door for applications to many astrophysically important neutron-rich nuclei, the obtained GT distribution points to shortcomings of the KB3 interaction family, which has been used to generate the weak-interaction library for iron-mass nuclei [14]. The KB3 interactions predict the GT strength to reside mainly in one strong state corresponding to the $f_{7/2}$ proton to $f_{5/2}$ neutron transition, while the data, in good agreement with shell model studies performed with Otsuka's GXPF1 interaction [15], show that the strength is distributed over several states. The authors attribute the difference between the two shell model calculations to the weaker spin-orbit and residual proton-neutron potentials found in the KB3 family.

At higher densities, when μ_e is sufficiently larger than the respective nuclear Q values, the capture rate becomes less sensitive to the detailed GT_+ distribution and depends practically only on the total GT strength. Thus, less sophisticated nuclear models might be sufficient. However, one is facing a nuclear structure problem which has been overcome only recently. Once the matter has become sufficiently neutron rich, nuclei with proton numbers $Z < 40$ and neutron numbers $N > 40$ will be quite abundant in the core. For such nuclei, Gamow-Teller transitions would be Pauli forbidden [16] (GT_+ transitions change a proton into a neutron in the same shell) were it not for nuclear correlation and finite temperature effects which move nucleons from the pf shell into the gds shell. To describe such effects in an appropriately large model space (e.g. the complete $fpgds$ shell) is currently only possible by means of the Shell Model Monte Carlo approach (SMMC) [17, 18]. In [19] SMMC-based electron capture rates have been calculated for more than 100 nuclei indicating that correlations across the $N = 40$ gap are quite effective

in unblocking GT_+ transitions making electron captures on nuclei, rather than on free protons, the dominant mode during the entire collapse.

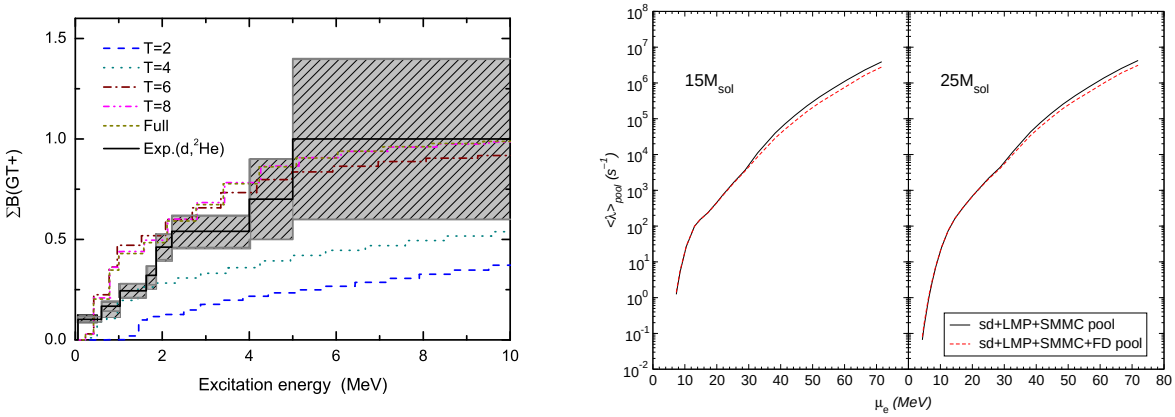

Figure 2. Left: Running GT_+ sum for different values of the particle-hole excitations across the $N = 40$ shell gap. The same normalization factor is applied to all the calculations and has been determined such as the total GT strength is reproduced by the full calculation. The experimental data are from [20]. (from [22]). Right: Comparison of NSE-averaged electron capture rates calculated for about 3000 individual nuclei (solid, see text) with those obtained for the restricted set of nuclei (dashed) considered in [19] (from [23]).

The prediction that cross-shell correlations unblock the GT_+ strength has recently been confirmed experimentally by a measurement for ^{76}Se (with Z=34 and N=42) [20]. This experiment revealed a B(GT) strength of 0.7±0.2 at excitation energies below 5 MeV in the daughter nucleus. This finding supplements indirect evidence derived from transfer reactions, which determined the neutron occupancy in the $g_{9/2}$ orbital of the ^{76}Se ground state as 5.8±0.3 in clear excess of the Independent Particle Model value of 2 [21]. In turn, there are nearly 4 neutron holes in the pf-shell unblocking GT_+ transitions for pf-shell protons. Furthermore the experiment identified also proton excitations across the $N = 40$ shell closure which can also contribute to the GT_+ strength via transitions to the $g_{9/2}$ and $g_{7/2}$ neutron orbitals. The experimental findings are well reproduced by large-scale shell model calculations [22]. These studies consider the (pf) orbitals for protons and the (p,$f_{5/2}, g_{9/2}$) orbitals for neutrons. Also the electron capture rates determined from the shell model and experimental GT_+ ground state distributions agree favorably well. If compared to the SMMC+RPA capture rates one finds a noticeable different temperature dependence at densities around 10^{10} g/cm^3, while the temperature dependence agrees nicely at higher densities ($> 10^{11}$ g/cm^3). This exemplifies an important fact: At densities, at which the electron chemical potential is comparable to the reaction Q-value, the capture rate is sensitive to the detailed GT_+ distribution. In turn, to properly describe these details nuclear models, like the large-scale shell model, are required which account for the relevant nuclear correlations. As the electron chemical potential grows faster with density than the average Q-value of the nuclei present, it suffices at higher densities that the total GT+ strength and its energy centroid are well described. This is fulfilled by the SMMC+RPA approach. This method however, does not account for all correlations needed to resolve the strength distribution at low excitation energies.

The shell model study for ^{76}Se clearly taught us that the convergence of cross-shell correlations is very slow requiring 6p-6h excitations or higher to properly describe the GT_+ distributions

(see Fig. 2). Such correlations are properly accounted for in the first step of the SMMC+RPA approach, which determines partial occupancies at finite temperature, but not in the second step, which uses these occupation numbers to derive capture rates within a rather simple RPA approach. Very recently interesting first steps have been taken to develop consistent models for the description of stellar models [28, 29]. So far these models consider up to 2p-2h excitations which, if compared to the shell model and SMMC+RPA approaches, are not sufficient to recover the unblocking of the GT_+ strength by cross-shell correlations. Hence these models need to be extended to include higher particle-hole correlations.

The right side of Fig. 2 compares the capture rate derived for the pool of more than 3000 nuclei (i.e. combining the rates from shell model diagonalization, SMMC, and from the parametrized approach) with those obtained purely on the basis of the shell model results. While the agreement is excellent at small electron chemical potentials (here the shell model rates dominate), the rates for the large pool are slightly smaller at higher μ_e values due the presence of neutron-rich heavy nuclei with smaller individual rates. Furthermore the new rates also include plasma screening effects which lead to an increase of the effective Q values and a reduction of the electron chemical potential, which both reduce the electron capture rates. The effect is rather mild and does not alter the conclusion that electron capture on nuclei dominates over capture on protons during the collapse.

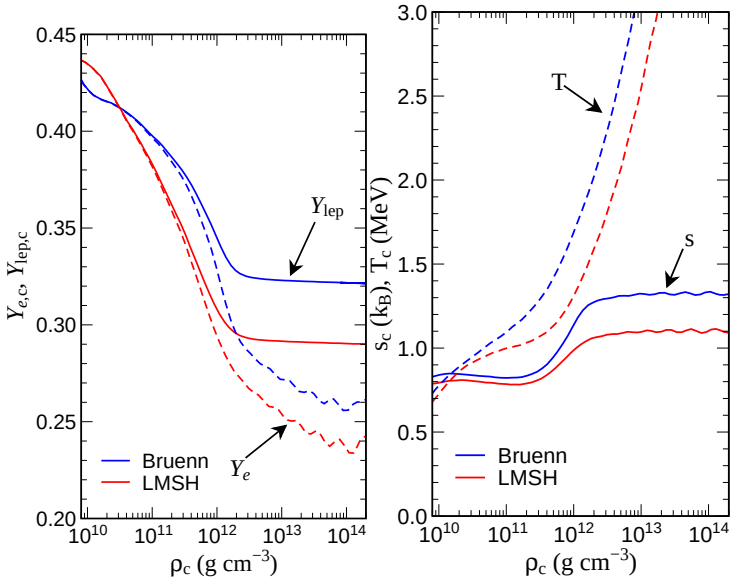

Figure 3. The electron and lepton fraction (left) and the temperature and entropy (right) in the center during the collapse phase. The thin lines are a simulation using the Bruenn parameterization [27], while the thick lines are for a simulation using the shell model rates [19]. (courtesy of Hans-Thomas Janka)

Shell model capture rates have significant impact on collapse simulations (see Fig. 3). In the presupernova phase ($\rho < 10^{10}$ g/cm^3) the captures proceed slower than assumed before and for a short period during silicon burning β-decays can compete [24, 25]. As a consequence, the core is cooler, more massive and less neutron rich before the final collapse. However, until recently simulations of this final collapse assumed that electron captures on nuclei are prohibited by the Pauli blocking mechanism, mentioned above. However, based on the SMMC calculations it has been shown in [19] that capture on nuclei dominates over capture on free protons. The changes compared to the previous simulations are significant [19, 26, 7]. Importantly the shock

is now created at a smaller radius with more infalling material to traverse, but also the density, temperature and entropy profiles are strongly modified [26].

The possibility to capture electrons on nuclei and free protons leads to a strong self-regulation during the collapse and it is observed that the collapse approaches the same core trajectory for stars between 11 and 25 solar masses before neutrino trapping and thermalization is reached at densities around 10^{12} g/cm^3 (Fig. 4, [7]). Thus it is expected that supernovae, independent of the stellar mass, have a quite similar neutrino burst spectrum. This spectrum, however, has also significantly changed after inelastic neutrino-nucleus reactions have been included in the simulations [30].

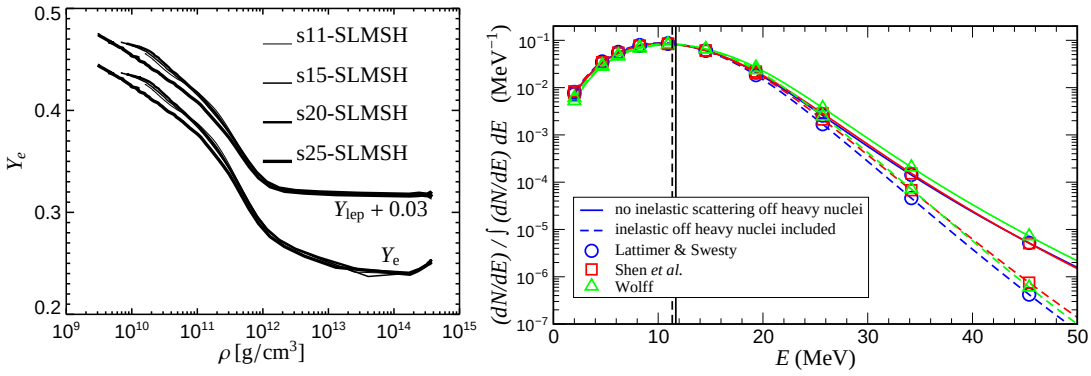

Figure 4. Left: The evolution of the electron-to-baryon ratio Y_e and the lepton-to-baryon ratio Y_{lep} as function of central density for stars with masses between 11 and 25 $M_\odot$. (from [7]). Right: Comparison of the normalized neutrino spectra, arising from the ν_e burst shortly after bounce, without (solid) and with (dashed) consideration of inelastic neutrino-nucleus scattering in the supernova simulations and for 3 different Equations of State. (from [30]).

4. Supernova nucleosynthesis

In a successful explosion the shock heats the matter it traverses, inducing an explosive nuclear burning on short time-scales. This explosive nucleosynthesis can alter the elemental abundance distributions in the inner (silicon, oxygen) shells. Recently explosive nucleosynthesis has been investigated consistently within supernova simulations. These studies found that in the early phase after the bounce the ejected matter is proton rich [31, 32, 33, 34], giving rise to a novel nucleosynthesis process (the νp-process [36]). In later stages, the matter becomes neutron rich [35] allowing for the r-process to occur.

4.1. The νp process

The freeze-out of proton-rich matter favors the production of α nuclei (^{4}He, ^{56}Ni, ^{64}Ge etc.), with some free protons left. In the supernova environment this freeze-out matter is subjected to extreme neutrino fluences. The neutrino energies are too small ($\langle E_{\nu_e} \rangle \approx 11$ MeV, $\langle E_{\bar{\nu_e}} \rangle \approx 15$ MeV) to induce sizable reaction rates on nucleons bound in nuclei. However, this is different for the free protons, which by anti-neutrino captures, can be converted to neutrons. This way a supply of free neutrons exists at rather late times during the nucleosynthesis process when heavy α nuclei like ^{56}Ni or ^{64}Ge are quite abundant. These nuclei have rather long life-times against weak decays and proton captures and would stop the matter-flow to even heavier nuclei. Due to the presence of free neutrons this is circumvented by (n,p) reactions, which act like β decays, and allow for the production of nuclides in the mass range $A \sim 80 - 100$ in the νp process, including the light p-isotopes ^{92,94}Mo and ^{96,98}Ru (see Fig. 5).

The synthesis of the heavy elements by the νp process depends sensitively on the $\bar{\nu}_e$ luminosity and spectrum which determine the late-time abundance of free neutrons. As has been shown recently [37, 38, 39], the $\bar{\nu}_e$ spectrum are affected by collective neutrino flavor oscillations which are expected to occur in the high-neutrino-density environment surrounding the neutron star [38] and can swap the $\bar{\nu}_e$ and $\bar{\nu}_{\mu,\tau}$ spectra above a certain split energy of order 15-20 MeV. Assuming such a swap scenario, Martinez-Pinedo *et al.* [40] have studied the impact of collective neutrino flavor oscillations on the νp process nucleosynthesis adopting anti-neutrino spectra from recent supernova simulations. The authors find that the oscillations increase the neutron abundance by enhanced electron anti-neutrino captures. The larger supply of neutrons boosts the matter flow to heavier nuclides and results in larger νp process abundances of nuclides with $A > 64$ (see Fig. 5).

4.2. The r-process

About half of the elements heavier than mass number $A \sim 60$ are made within the r-process, a sequence of rapid neutron captures and β decays. The process occurs in environments with extremely high neutron densities [41]. Then neutron captures are much faster than the competing decays and the r-process path runs through very neutron-rich, unstable nuclei. Once the neutron source ceases, the process stops and the produced nuclides decay towards stability producing the neutronrich heavier elements.

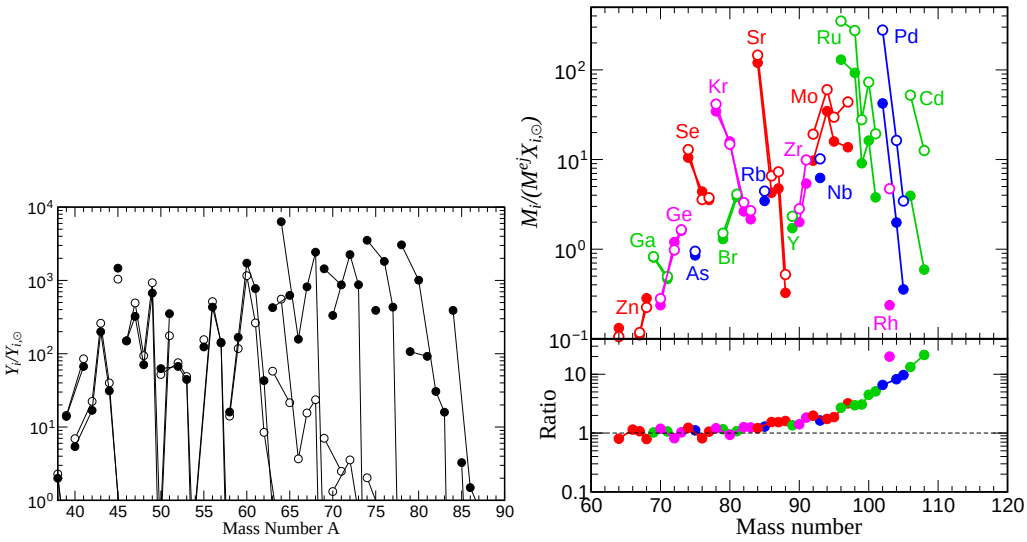

Figure 5. Left: Elemental abundance yields (normalized to solar) for elements produced in the protonrich environment shortly after the supernova shock formation. The matter flow stops at nuclei like ^{56}Ni and ^{64}Ge (open circles), but can proceed to heavier elements if neutrino reactions are included during the network (full circles) (from [36]. Right: Abundances of νp nucleosynthesis calculations with (open circles) and without (full circles) considering the effects of collective neutrino flavor oscillations (normalized to solar). The lower panel shows the ratios for the two nucleosynthesis studies as function of mass number.

Despite many promising attempts the actual site of the r-process has not been identified yet. However, parameter studies have given clear evidence that the observed r-process abundances cannot be reproduced at one site with constant temperature and neutron density [42]. Thus the abundances require a superposition of several (at least three) r-process components. This likely implies a dynamical r-process in an environment in which the conditions change during

the duration of the process. The currently favored r-process sites (core-collapse supernovae [43] and neutron-star mergers [44]) offer such dynamical scenarios. However, recent meteoritic clues might even point to more than one distinct site for our solar r-process abundance [45]. The same conclusion can be derived from the observation of r-process abundances in low-metallicity stars [46], a milestone of r-process research.

Support by the Helmholtz Alliance EMMI, the SFB 634 of the Deutsche Forschungsgemeinschaft and by the Helmholtz International Center for FAIR is gratefully acknowledged as is the collaboration with many colleagues, in particular with Gabriel Martínez-Pinedo.

[1] Adelberger E G *et al.* 1998, *Rev. Mod. Phys.* **70** 1265
[2] Adelberger E G *et al.* 2011, *Rev. Mod. Phys.* **83** 195
[3] Raiola F. *et al.* 2002, *Phys. Lett.* B **547** 193
[4] Pizzone R G *et al.* 2003, *Nucl. Phys.* A **718** 496c
[5] Assenbaum H J, Langanke K and Rolfs C E 1987, *Z. Phys.* A **327** 461
[6] Bethe H A 1990, *Rev. Mod. Phys.* **62** 801
[7] Janka H-Th *et al.* 2007, *Phys. Rep.* **442** 38
[8] Caurier E, Langanke K, Martínez-Pinedo G and Nowacki F 1999, *Nucl. Phys.* A **653** 439
[9] Langanke K and Martínez-Pinedo G 2000, *Nucl. Phys.* **A673** 481
[10] Frekers D 2006, *Prog. Part. Nucl. Phys.* **57** 217
[11] Langanke K and Martinez-Pinedo G 2003, *Rev. Mod. Phys.* **75** 819
[12] Bäumer C *et al.* 2003, *Phys. Rev.* C **68** 031303(R)
[13] Sasano M *et al.* 2011, *Phys. Rev. Lett* in print
[14] Langanke K and Martinez-Pinedo G 2001, *At. Data Nucl. Data Tables* **79** 1
[15] Honma M, Otsuka T, Brown B A and Mizusaki T 2004, *Phys. Rev.* C **69** 034335
[16] Fuller G M 1982, *Astr. J.* **252** 741
[17] Langanke K *et al.* 1995, *Phys. Rev.* C **52** 718
[18] Koonin S E, Dean D J and Langanke K 1997, *Phys. Rep.* (1997) 2
[19] Langanke K 2003 *et al.*, *Phys. Rev. Lett.* **90** 241102
[20] Grewe E W *et al.* 2008, *Phys. Rev.* C **78** 044301
[21] Kay B P *et al.* 2009, *Phys. Rev.* C **79** 021301
[22] Zhi Q *et al.* 2011, *Nucl. Phys.* A **859** 172
[23] Juodagalvis A *et al* 2010, *Nucl. Phys.* A **848** 454
[24] Heger A *et al.* 2001, *Phys. Rev. Lett.* **86** 1678
[25] Heger A *et al.* 2001, *Astr. J.* **560** 307
[26] Hix R W *et al.* 2003, *Phys. Rev. Lett.* **91** 210102
[27] Bruenn S W 1985, *Astr. J. Suppl.* **58** 771
[28] Paar N, Colo G, Khan E and Vretenar D 2009, *Phys. Rev.* C **80** 055801
[29] Dzhioev A A *et al.* 2010, *Phys. Rev.* C **81** 015804
[30] Langanke K *et al.* 2008, *Phys. Rev. Lett.* **100** 011101
[31] Thielemann F.-K. *et al.* 2003, *Nucl. Phys.* A **718** 139c
[32] Pruet J *et al.* 2005, *Astr. J.* **623** 1
[33] Fröhlich C *et al.* 2006, *Astr. J.* **637** 415
[34] Fischer T *et al.* 2010, *A&A* **517** 180
[35] Wanajo S 2006, *Astr. J.* **647** 1323
[36] Fröhlich C *et al.* 2006, *Phys. Rev. Lett.* **96** 142502
[37] Dasgupta B, Dighe A, Raffelt G G and Smirnov A Y 2009, *Phys. Rev. Lett.* **103** 051105
[38] Duan H, Fuller G M and Qian Y 2010, *Ann. Rev. Nucl. Part. Sci.* **60** 569
[39] Duan H, Friedland A, McLaughlin G C and Surman R. 2011, *J. Phys.* G **38** 035201
[40] Martinez-Pinedo G *et al.* 2011, *Eur. Phys. J.* A **47** 98
[41] Cowan J J, Thielemann F-K and Truran J W 1991, *Phys. Rep.* **208** 267
[42] Kratz K L *et al.* 1993, *Astr.J.* **402** 216
[43] Woosley S E *et al.* 1994, *Astr. J.* **399** 229
[44] Freiburghaus C, Rosswog S and Thielemann F-K 1999, *Astr. J.* **525** L121
[45] Wasserburg G J , Busso M, Gallino R and Nollett K M 2006, *Nucl. Phys.* A **777** 5
[46] Sneden C *et al.* 2003, *Astr. J.* **591** 936